Computer Modeling of α- to β′-form Phase Transitions Using Theoretical Triglyceride Structures

James W. Hagemann* and **John A. Rothfus**
Northern Regional Research Center, ARS/USDA, 1815 N. University St., Peoria, IL 61604

Intermolecular energy calculations were performed on theoretical triarachidin α-form structures as selected bond rotations converted them into β′-forms with a chain-tilt change in the glycerol region. Interactions across the methyl gaps amounted to only 2–3% of the total energy in initial α- and final β′-forms, but computer-generated energy profiles during α- to β′-phase transitions revealed highly repulsive regions due to the close approach of methyl groups. This methyl gap interaction, plus additional repulsive interactions in the lateral packing of molecules during rigid chain rotations, necessitated modification of certain chain movements during phase transition to reduce excessive repulsive energy. These results suggest that phase transitions proceed in a particular sequence of events that either distribute energy to promote further phase excitation or that lead to collapse into the stable polymorphic form. Phase transition energy curves also reveal that secondary α- and β′-forms are possible and are dependent on the starting α-forms, the direction of chain rotation and the subcell arrangement.

In recent publications (1,2), studies were reported on conformational structures and packing arrangements of theoretical monoacid triglyceride molecules in α- and β′-forms in which computer modeling was used. These studies on the lowest and intermediate melting polymorphs were among the first to use intermolecular energy calculations to examine triglyceride packing arrangements. Computer modeling had been used previously for intramolecular conformational analyses of phospholipids (3) and short-chain triglycerides (4,5) and, only more recently, for a combination of intra- and intermolecular interactions for phospholipid conformations (6). Rapid conversion upon heating of α-forms into β′-forms or the highest melting β-form (7) necessitates use of techniques other than conventional x-ray diffraction (8–10) or thermal analysis (9,11,12). Computer modeling is well-suited for examining these fluctuating polymorphic forms and associated transformation processes.

Computation of atom-atom interactions during the α- to β′-form transformation is a logical extension from analyses of packing energies for the α- and β′-forms (1,2). Intermolecular minimization procedures thus far indicate that, for theoretical α- and bent β′-form (13) structures, several equally preferred structure-subcell arrangement combinations are possible. For α-forms, subcell arrangement had a greater effect on packing energy than did the configuration of the triglyceride. This was also quite true for bent β′-forms, where several subcell arrangements revealed unsymmetrical packing. Useful understanding of lipid phase behavior requires knowledge of both individual crystalline forms and the atomic-level mechanics that obtain during changes between forms. Therefore, a theoretical pathway for α- to β′-form phase transition was modeled with previously determined subcell packings to examine the effect of triglyceride conformation and subcell arrangement on the transition energy profile.

*To whom correspondence should be addressed.

EXPERIMENTAL

The eight starting triarachidin α-form configurations used were those described in (1). Briefly, the triarachidin model was constructed with the central glycerol carbon located at X = 0, Y = 0 in a Cartesian coordinate system. Chain #1 intersects the X-Y plane along the +X-axis and chain #3 intersects the X-Y plane along the -X-axis. The long dimension of the molecule is parallel with the Z-axis. The bent β′-forms, to which the α-forms transformed, were as described in (2), but due to the unsymmetrical packing found in some β′-form subcell arrangements, only four preferred arrangements (2), were used in this study. Subcell positions for the starting α-forms and ending β′-forms were as determined previously (1,2). Oscillatory motion about the long hydrocarbon chain axis was not incorporated into α-form structures.

Rotation about bonds required to change an α-form into a bent β′-form (2) and differences between X-, Y- and Z-axis translation values i.e., amount of whole-molecule movement on each axis from molecule P (2), for starting α-forms and ending β′-forms were divided into 200 steps. At each step, intermolecular energy calculations were performed for pairs of triglyceride molecules by using the semi-empirical potentials of Coiro et al. (14), which do not include dipole interactions. The pairs consisted of a central molecule, molecule P, and a molecule in each of the six positions around molecule P (2). In addition, calculations were performed to quantitate interactions between parts of eight molecules across the methyl gaps for a total of 14 molecular positions around molecule P. Curves were drawn for the interaction energy vs. step for each position, and the energies of all positions were summed for a total energy curve. Bond rotations and translation shifts were complete by step 192, so bonds in the molecule could be rotated slightly beyond the β′-form to check for development of further energy minima.

A flow diagram of the Fortran IV computer program used to determine the 14 position energy curves and the final total curve is shown in Figure 1. Parts of the diagram are explained in a later section of this paper. Because the rotated bonds were on the chain 2 (15) side of the molecule, the entire molecule was tilted about the X-axis through the central glycerol carbon so that in the final β′-form the methyl groups on chains 1 and 3 were approximately in line on the X-axis with the methyl group on chain 2. The central molecule was aligned thusly after each incremental step in bond rotation. After the incremental bond rotations, tilting of the molecule, and calculation of X-, Y- and Z-axis translation shifts, the second molecule was built by using a

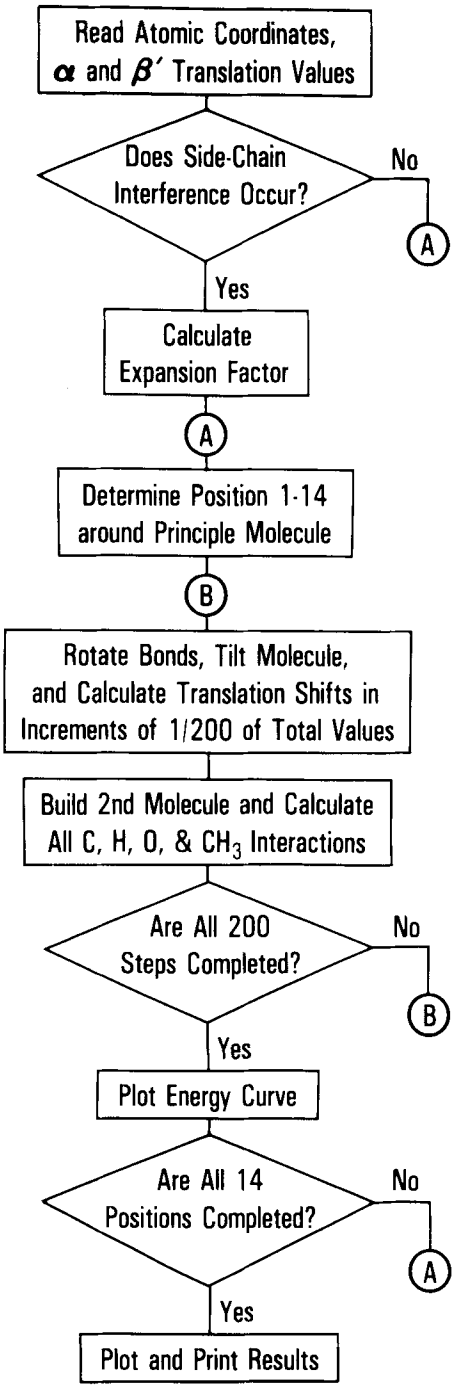

FIG. 1. Flow diagram of computer program for calculation of interaction energies between pairs of oscillating triglyceride molecules during α- to β'-form transition. See section on interactions in chain packing for explanation of X-bloom expansion factor.

symmetry operation determined from the best energy minimum of prior results.

RESULTS

The hydrocarbon chain subcell packing in triglyceride α- and β'-forms (10) is slightly different because individual zigzag chain planes alternate in successive rows in

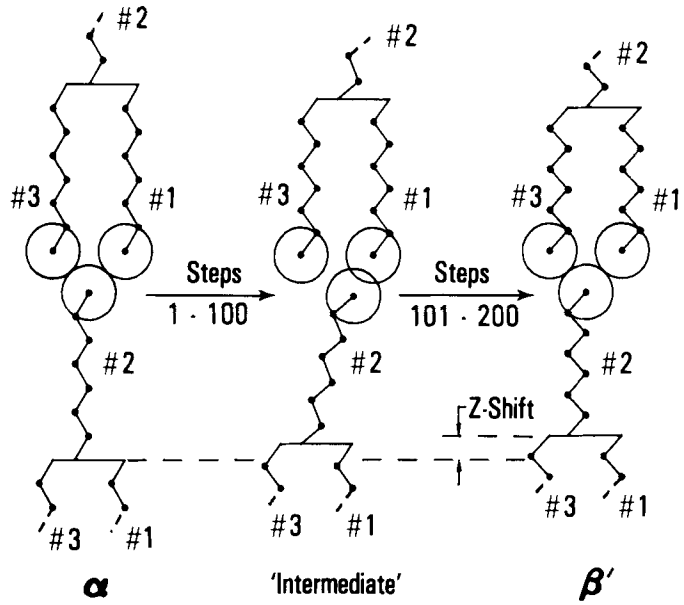

FIG. 2. Interactions across methyl gap. Chains are numbered according to the convention of Lutton (15). Carbon atoms are solid circles; hydrogen atoms are not shown. Large open circles represent 2 Å Van der Waals radii around methyl groups. Chains are shortened for reasons of space, and details of glycerol regions are not shown.

β'-forms but are random in α-forms due to oscillatory motion about the long-chain axes (16). To simplify computations, the starting α-form zigzag patterns were based on β'-form subcells, which have rows of parallel zigzag planes with alternating zigzag planes in successive rows. The α-form triglycerides were all symmetrical tuning-fork molecules with alternating upright and inverted molecules in each horizontal row. Also, chains 1 and 3 were placed in the same subcell row, and hydrocarbon portions of the chains were in the all *trans* conformation during the transition.

Interactions across methyl gaps. Interaction energy across the methyl gaps in α- and β'-forms amounted to only 2-3% of the total interaction energy (1,2), but a high repulsive energy region was found in the methyl gap energy computations during the α- to β'-transition. Reasons for this repulsive energy region are illustrated in Figure 2, in which chains are numbered according to the convention of Lutton (15) and circles represent the two-Å Van der Waals radii of methyl groups. During rotation of the two or three bonds to make the β'-form, chain 2 swings out slightly from between chains 1 and 3. Computer simulations of this movement reveal overlap of Van der Waals radii. This problem is complicated by a requirement that the long spacing be shortened during the α- to β'-form transition. Overall, the #2 chain end must move closer to the #1 and #3 chain ends in the Z-axis direction to have a four-Å spacing between methyl groups of β'-form molecules. The Van der Waals radii of methyl groups are two Å, and it is assumed that close packing will occur. By slowing the change from α- to β'-form Z-axis translation values, the difference referred to as Z-shift in Figure 2, much of the

overlap could be eliminated. This was accomplished by expressing the Z-shift as the exponential function

$$\text{Z-shift} = (\text{ZZ-ZS})/191^2 \times (\text{STEP No.} - 1)^2$$

where ZS = starting α-form Z-axis translation value and ZZ = ending β'-form Z-axis translation value. This function, in effect, delayed the Z-shift until the rotated chain began to move back to a vertical position. As shown in Figure 3, for a C_{20}-U structure having nonparallel chains, carbonyl left and opposite zigzag on chains 1 and 3 (2), the original methyl gap energy curve has a transition energy of 140 Kcal/mol around step 80, but after delaying the Z-shift the maximum was only a little over two Kcal/mol.

The extent to which this methyl gap adjustment affected the energy was influenced greatly by the arrangement at the methyl gap. For structures having nonparallel chains, the energy curves for both alternating and nonalternating angles of tilt (2) at the methyl gap differed only slightly in magnitude and pattern. Most noticeable were the pattern and magnitude of the energy difference for a parallel chain structure, represented in Figure 4 by a C_{20}-D structure having the carbonyl group to the left with opposite zigzags on chains 1 and 3. When the angle of tilt did not change at the methyl gap, the energy curve was smooth with the maximum of 6.5 Kcal/mol occurring early in the transition around step 60. For a change of tilt at the methyl gap the energy curve remained attractive (negative) through-

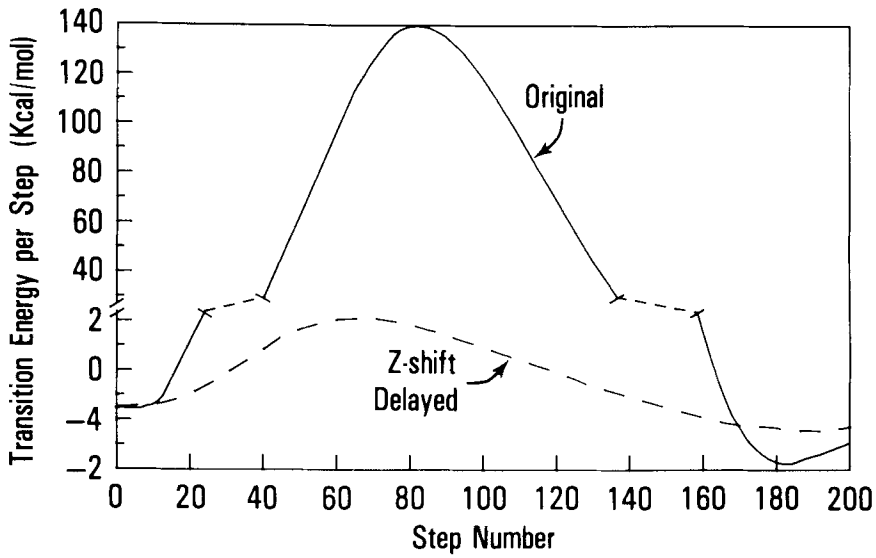

FIG. 3. Adjustment for methyl gap interactions. Each step represents 1/200 of transitions shift parameters. Starting α-form is at Step 0 and final β'-form at Step 192.

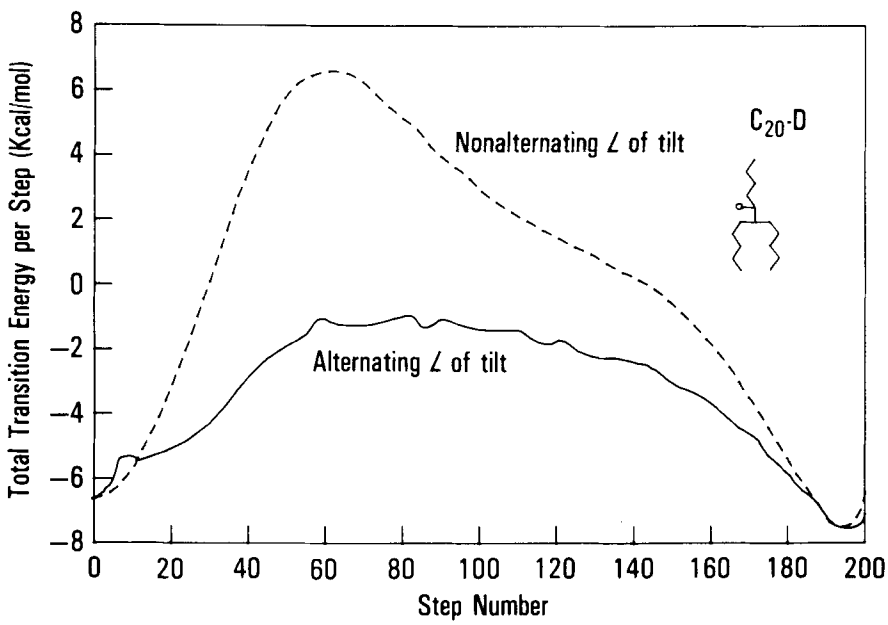

FIG. 4. Effect of methyl group orientation on energy curves at the methyl gap.

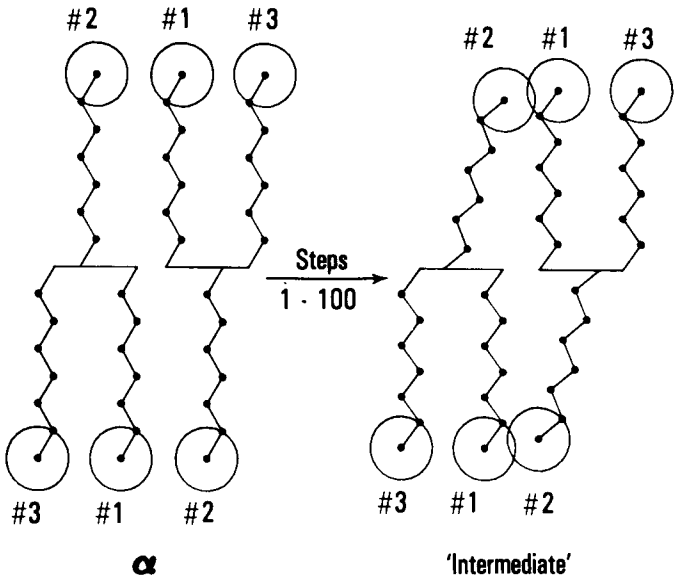

FIG. 5. Interactions in chain packing. Chains are numbered according to the convention of Lutton (15). Carbon atoms are solid circles; hydrogen atoms are not shown. Large open circles represent 2 Å Van der Waals radii around methyl groups. Chains are shortened for reasons of space, and details of glycerol regions are not shown.

out the 200 steps being relatively flat but with minor undulations over the central steps of the calculations.

Interactions in chain packing. In a similar manner, movement of chain 2 also caused a close approach of methyl groups (Fig. 5) in side by side molecules, which produced a high repulsive energy region. The extent of this repulsive region was dependent on the starting X-axis translation values with methyl groups approaching as close as 1.8 Å in some situations. To reduce the large repulsive energy, an X-bloom expansion factor (Fig. 1) was introduced to move the second molecule away from the principle molecule, P (2), over the central steps of the calculations. The X-bloom factor was determined by making a preliminary run through the 200 steps, without energy calculations or plotting, to find the minimum approach distance of the methyl groups. The difference between the minimum approach distance and 3.5 Å, slightly less than double the Van der Waals distance, is the X-bloom factor. The amount of change in the X-direction, X-shift, was expressed as a sine wave function so that the maximum movement would occur around step 100. This X-shift, in addition to the translational change, was calculated as

$$\text{X-shift} = (\text{XX-XS})\,[(\text{STEP No.} - 1)/191] \pm [\text{X-BLOOM} \times \text{SIN}\,(0.9375 \times \text{STEP No.})]$$

where XS = starting α-form X-axis translation value, XX = ending β'-form X-axis translation value, and the value 0.9375 = a factor to give maximum displacement in the central portion of the curve and no displacement at step 192. The plus or minus choice allows movement of inverted molecules in positions 1 and 4 (2) in a positive X-direction and molecules in outer positions 2 and 6 in a negative X-direction. The curves shown in Figure 6 are an example of a subcell arrangement where side-chain packing interference occurred between the principle molecule, P, and subcell position 1. The original curve shows over 600 Kcal/mol around step 90, which reduced to 10 Kcal/mol after applying the X-bloom adjustment factor. Even though subcell position 4 was moved in the +X-direction, the repulsive interference with molecule P was in the order of the X-bloomed curve in Figure 6 when the X-bloom factor was subtracted from 3.5 Å. However, when the X-bloom factor was subtracted from twice the methyl group Van der Waals radii, four Å, the repulsive energy was quite high. The term X-bloom minus 3.5 Å was chosen to balance the amount of repulsive energy on either side of molecule P.

Effect of conformation on transition energy. Effects due to conformation and to subcell arrangement on transition energy cannot be entirely divorced, but more variation occurred between different conformations than

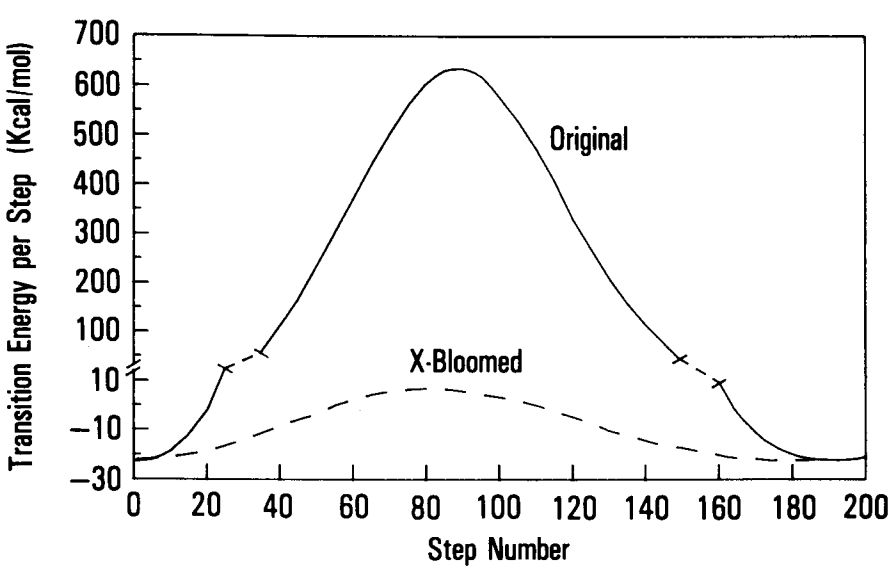

FIG. 6. Adjustment for chain packing. Each step represents 1/200 of transition shift parameters. Starting α-form is at Step 0 and final β'-form at Step 192.

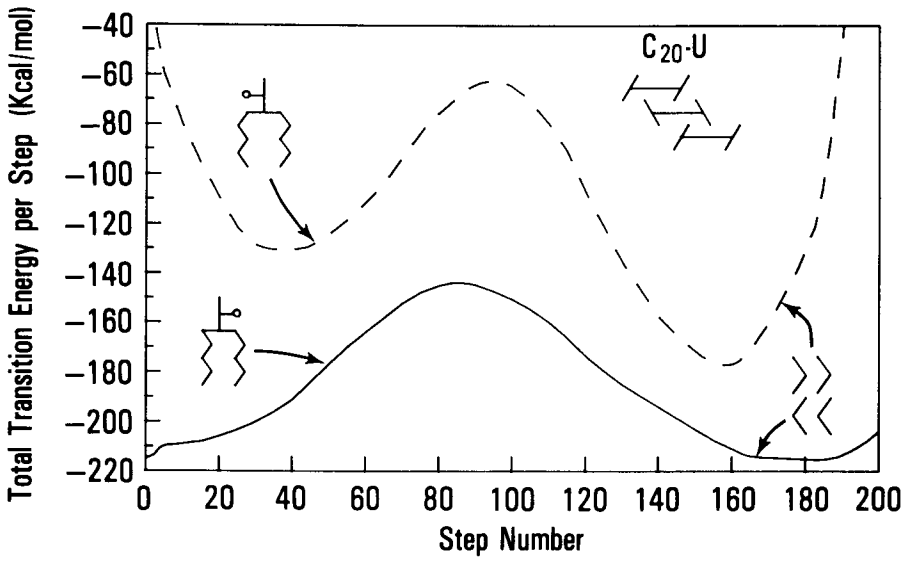

FIG. 7. Effect of structure on transition energy. Curves represent sums of energies computed for interactions between a central subcell molecule and molecules in 14 adjacent positions. Inserts at upper and lower right indicate three upright molecules in subcell and methyl gap orientation, respectively. Inserts at upper and lower left symbolize the triglyceride structure. Each step represents 1/200 of transition shift parameters. Starting α-form is at Step 0 and final β'-form at Step 192.

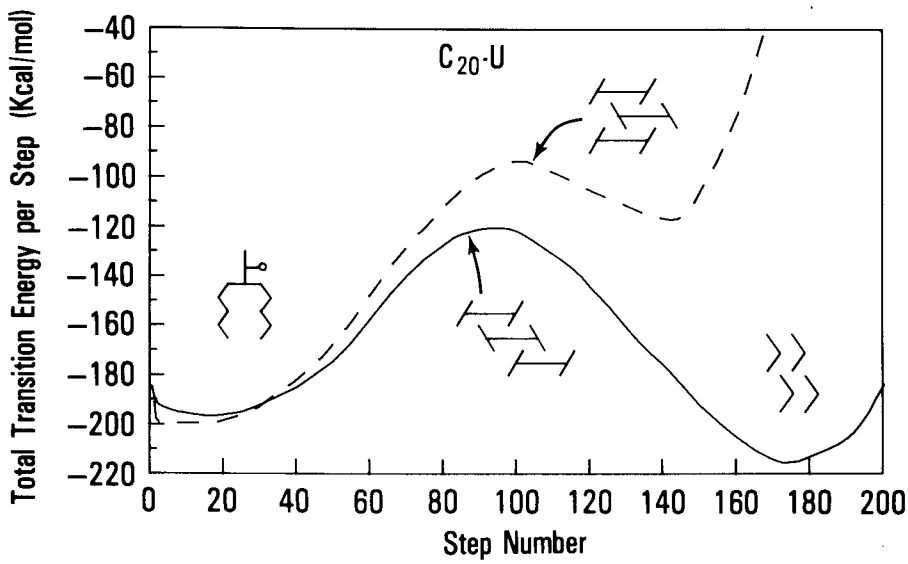

FIG. 8. Effect of subcell arrangement on transition energy. Lower right insert represents methyl gap orientation. Subcells are each indicated by three upright molecules. Insert at lower left symbolizes the triglyceride structure. Each step represents 1/200 of transition shift parameters. Starting α-form is at Step 0 and final β'-form at Step 192.

between the four subcell arrangements of any one structure. A majority of the curves fell into two general types as illustrated in Figure 7, which depicts results for different triglyceride conformations in one of the four preferred subcell arrangements shown in (2) and Table 1 and with the same nonalternating configuration. Both structures were designated β'-U in (2).

The dashed curve representing the conformation with opposite zigzag patterns in chains 1 and 3 shows a minimum near step 40, which presumably represents a secondary α-form, because at that point molecular conformation has changed only slightly from the starting α-form. The structure at step 40 is nearly vertical with an angle of tilt of about 85°. The structure represented by the minimum at approximately step 160 has a long spacing about 1.6 Å longer than the reported β'-form of triarachidin (9). The minimum at step 160 also has a greater negative energy value than that at step 40, which is to be expected for β'-forms.

An α-form minimum was not observed for the solid curve while the β'-region is quite flat from about steps 170 to 190. This suggests many forms of about equal

TABLE 1

Energies and Calculated Long Spacings of Secondary α- and β'-forms from Energy Curve Profiles[a]

Subcell structure from (2)	Same zigzag		Opposite zigzag		Same zigzag		Opposite zigzag	
	α	β'	α	β'	α	β'	α	β'
	C_{20}-D[b]							
	Parallel chains, carbonyl left on chain 2				Nonparallel chains, carbonyl right on chain 2			
1	-	-164.6 (50.7)	-159.1 (55.7)	-130.3 (50.8)	-	-172.2 (50.6)	-204.2 (55.7)	-
2	-	-	-157.9 (55.7)	-12535.0 (53.3)	-	-	-189.3 (55.7)	-12559.0 (51.6)
3	-	-	-145.6 (55.7)	+562.1 (51.5)	-	-	-196.7 (55.7)	-2905.0 (52.5)
4	-	-	-	-13627.0 (53.3)	-	-167.5 (50.9)	-196.8 (55.7)	-17499.0 (51.5)
	C_{20}-U[b]							
	Nonparallel chains, carbonyl left on chain 2				Nonparallel chains, carbonyl right on chain 2			
1	-	-190.1 (51.3)	-166.8 (55.7)	-196.6 (52.3)	-	-201.4 (50.7)	-	-109.0 (54.4)
2	-182.1 (55.7)	-191.5 (50.7)	-131.2 (55.6)	-177.3 (52.3)	-	-216.0 (51.5)	-197.3 (55.7)	-216.3 (51.6)
3	-189.8 (55.7)	-198.7 (51.3)	-152.0 (55.6)	-191.4 (52.3)	-	-212.4 (50.7)	-202.8 (55.7)	-146.0 (53.6)
4	-187.9 (55.7)	-182.8 (50.7)	-137.5 (55.6)	-184.6 (51.9)	-	-205.7 (50.7)	-	-126.5 (53.4)

[a]Interaction energies are expressed in Kcal/mol. Numbers in ( ) are the calculated long spacings expressed in Å. Literature values for X-ray long spacings of triarachidin α- and β'-forms are 55.8 and 50.7 Å, respectively (9).
[b]See reference (2) for explanation of β'-form structures.

energy over a change in long spacing distance of about 1.2 Å.

Effect of subcell arrangement on transition energy. Energy curves for different subcell arrangements of the same structure displayed very little variability. One example of difference is shown in Figure 8 for a triarachidin structure with nonparallel chains (C_{20}-U). Profiles of the two curves are similar, but the positions and energy levels of minima in the β'-region are quite different. The dotted curve, representing an unsymmetrical subcell, has a minimum around step 145 with an energy value of -115 Kcal/mol which is much lower than the starting α-form energy. This minimum is also quite far removed from the β'-form at step 192 and has a long spacing considerably greater than the literature value. In contrast, the solid curve shows a minimum around step 175 and an inflection at step 192 consistent with the transition ending β'-form. Only a very minor secondary α-form minimum was observed in each of the curves.

Because triglycerides may occur as mixtures of different subcell arrangements, energy curves also were obtained for the average of the four preferred β'-form arrangements (2). Average curves of the four subcells for the two structures in Figure 7 are very similar to the curves displayed except for small minima on the dashed curve at approximately steps 170 and 180.

A summary of results for the various structure/subcell

arrangements with nonalternating methyl gap configurations is reported in Table 1.

The calculated long spacing for the secondary α-form from the dotted curve in Figure 7 is 55.6 Å. This is just 0.2 Å less than the reported x-ray long spacing of 55.8 Å (9) and represents an angle of tilt of about 85°. Other secondary α-form minima are reported with calculated long spacings of about 55.7 Å. These minima generally occurred between steps 5 and 20 of the energy profile curve and therefore have angles of tilt only a few degrees less than the 90° of the starting α-form.

Long spacings for the secondary β'-forms in Table 1 ranged from 54.4 Å to the expected x-ray long spacing (9) of 50.7 Å. It may be questionable whether some of these forms should be called β'. The 54.4 Å long spacing for one form of the C_{20}-U structures is only 1.3 Å removed from that of the α-form. The tentative β' designation is based on the fact that the energy minima occurred beyond the midpoint, or step 100, of the energy profile curve for the α to β' transition. Multiple β'-form minimal generally were not observed, but curves were often quite flat in the β'-region; e.g., the solid curve in Figure 7. Results reported in Table 1 for curves with broad β' regions represent computer output at the step for which attractive energy value is greatest. Results for the curves of Figure 8 do not appear in Table 1. Only nonalternating angle of tilt configurations are reported because methyl gap energy had little influence on final curves after Z-shift adjustment (Fig. 3).

For a number of the subcell arrangements previously reported (2), total interaction energy values were extremely attractive or repulsive depending on the placement of some of the molecules around the central principle molecule. Such arrangements also caused energy curve values to deviate excessively for some of the opposite zigzag conformers of C_{20}-D, and they eliminated entirely α- or β'-form minima for several of the same zigzag conformers. An example of this curve is shown in Figure 9 for the average of all four subcell arrangements for a C_{20}-D structure having nonparallel chains, carbonyl right and an opposite zigzag pattern. The α-form minima in Table 1 for this structure do not appear in Figure 9 because of their small size relative to β'-form minima. Structure/subcell arrangement combinations yielding curves without α- or β'-form minima also were encountered. They generally sloped in the repulsive energy direction (+) from the starting α-form to step 200. The absence of a β'-form minimum at step 192 in some of the curves of Figures 7–9 is also due to the positioning of the molecule in the starting subcell arrangement.

DISCUSSION

Intermolecular and intramolecular interactions can both, obviously, affect molecular packing, which in turn determines the transformation paths available to polymorphic solids. Ideally both types of interactions should be optimized in a search for transformation paths that follow energy minima. Ultimately such unconstrained modeling may be practical. Current limits on computer time and capacity, however, compelled us in these initial studies to consider the consequences of intermolecular interactions with the expectation that doing so would help to envision critical aspects of the intramolecular interactions already examined.

The results described above represent several of many theoretical possibilities for conversion of α- into β'-forms. The starting α-forms are somewhat symmetrical with chains 1 and 3 approximately equidistant from the extended long axis of chain 2 and with methyl groups of chains 1 and 3 aligned. This conformation is in contrast to one recently proposed for the α-form (17) in which chain 3 is a shortened side chain similar to that in the β-form (7). Concerning the β'-form structure, controversy exists as to whether alternation of chain tilt takes place within the glycerol region (13) or at the

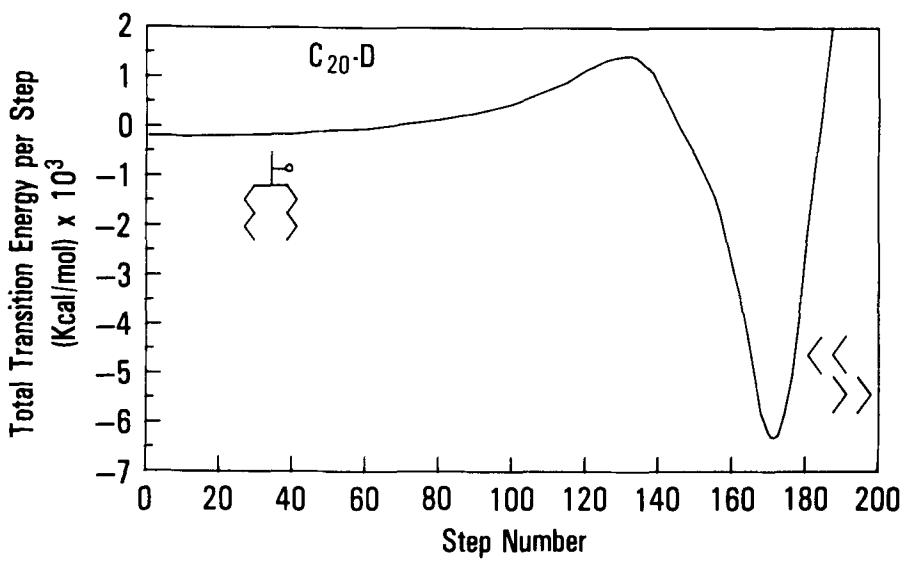

FIG. 9. Average energy curve of four subcell arrangements. Inserts at lower right and upper left represent methyl gap orientation and triglyceride structure, respectively. Each step represents 1/200 of transition shift parameters. Starting α-form is at Step 0 and final β'-form at Step 192.

methyl end group plane (17). Therein lies the complexity of the problem; uncertainty of either the initial α- or final β'-form structures.

In the absence of immutable evidence for a specific conformation in the glycerol region, a symmetrical α-form was chosen as a logical initial monomeric condensation product from the population of dissociated random conformers in a triglyceride melt. And, because even chainlength β-forms possess no change of chain tilt at the methyl end group plane (7), consistency with x-ray data was maintained by using β'-form structures bent in the glycerol region.

At some point in the liquid $\rightarrow \alpha \rightarrow \beta' \rightarrow \beta$ conversion process, side-chain character must be assumed by chain 3 and change of chain tilt eliminated to comply with β-form structure requirements (10). From DSC scans (12), it is evident that a greater molecular event occurs in the $\alpha \rightarrow \beta'$ transition than in the $\beta' \rightarrow \beta$ transition. For experimental purposes, we assume that this event is a change from no chain tilt to chain tilt in the glycerol region. The proposal that chain tilt occurs at the methyl end group region (17) is based on data from an odd chainlength triglyceride which may or may not be the same for even chainlengths. It merits examination in a later analysis. Many differences exist between odds and evens based on thermal analysis (12) and x-ray long spacing (9) data. Projections from one to the other are at best tentative.

Whereas β'-forms are higher melting and exhibit greater heats of fusion than α-forms, it seems reasonable that computed interaction energies for β'-forms should also be higher. For certain subcell structures in Table 1, interaction energies of β'-forms are about equal to or less than those of α-forms. Such subcell structures would, therefore, be unlikely in the α --> β' conversion process. They might be more favorable for longer or shorter chainlengths, mixed chainlengths, or impure materials.

Minima listed in Table 1 cannot be classified by the usual method of x-ray short spacings (16), so it is impossible to tell where in the transition α-forms cease to exist and β'-forms begin. Secondary α-forms represented by minima in the energy profile curves are only a few degrees from vertical. They are consistent with multiple α-forms that have been observed by thermal analysis of saturated monoacid triglycerides with chainlengths of C_{22} and greater (12). They suggest mechanistic subtleties that most analytical techniques will not detect in lipid transitions.

X-ray data are not available to verify multiple α-forms, but long spacings were reported recently for two β'-forms of trimargarin and tristearin (18). The two β'-forms of trimargarin differed by 0.5 Å; those of tristearin by 1.0 Å. For triarachidin, the next longer member in the homologous series of even chainlengths, the difference in β'-long spacings should approximate that of tristearin. Several of the secondary β'-forms in Table 1 have calculated long spacings that are 0.8-0.9 Å longer than the x-ray value of 50.7 Å for triarachidin (9). Three of the C_{20}-D structure/subcell combinations have β'-long spacings in this range, but all have excessive (positive or negative) energy values. With slight adjustment of molecular positions in the subcell, energy values could conform to more standard values. One of the C_{20}-U carbonyl right structures (opposite zigzag) in subcell 2 does not need adjustment because it has a very strong β'-form minimum 0.9 Å longer than the x-ray value. The similar structure having a same zigzag pattern had an almost identical energy value and a calculated long spacing 0.1 Å less. Two of the C_{20}-U carbonyl left structures (same zigzag) in subcell arrangements 1 and 3 have β'-forms 0.6 Å greater than the x-ray value. Models of these structures all appear identical and conform with the previous speculation that the differences between the β'-forms may be due to very minor lateral packing rearrangements of the hydrocarbon chains (19).

Considerable oscillation present in the α-form (16) results in a random orientation of chain planes. This concept seems evident from results in Table 1. Three of the four structures showed no secondary α-forms when chains 1 and 3 had the same zigzag pattern. The majority of α-forms occurred in structures having the opposite zigzag pattern, which is more in agreement with the idea of random chain orientations. Likewise, the same zigzag configuration for the single all parallel chain structure produced but one β'-form. Such findings, that results conform to known crystal structure concepts, enhance confidence in computer modeling techniques.

Raman spectra for polymorphic phases of triglycerides disclose differences in methyl group regions (18). These results reflect conditions in defined structures but allow little insight into events during transitions between phases. Prior modeling results (1,2) had shown that the energy of the methyl group region amounted to only 2-3% of the total overall interaction energy. But during rotation of rigid chain 2, overlap of methyl group Van der Waals radii caused excessive repulsive energy. The methyl group region could thus play a major role in phase transitions, perhaps more so than glycerol and adjacent hydrocarbon regions, which remain relatively static in the present model. Atoms in and near glycerol undoubtedly move during transitions that shorten the x-ray long spacing, but synchronous movements in this region could allow change with less nearest neighbor interaction than would likely occur at the ends of rotating chains (chain 2 in the model).

Methyl group repulsion and side chain interference that affected the results of this study were found by computation for molecules transformed by rotation of rigid chains. If polymorphic transformations proceed along minimum energy paths, adjustments to rigid chain movement could reduce transition barriers to acceptable levels. It cannot be stated with certainty, however, that the global minimum pathway was achieved with the described motion. Other types of motion by which effective bond rotation is accomplished incrementally with small dislocations transmitted down the chain, perhaps a crankshaft type motion, might result in less Van der Waals overlap. Such situations remain for subsequent examination. For example, our functions for X- and Z-translations to relieve Van der Waals overlaps are arbitrary. Other translations might be equally effective in reducing repulsive interactions. For the present, adjustments made in methyl group and side chain movements to accommodate repulsive energies are not unlike dimensional shifts typical of transforming lipids. The need for such adjustments and the observation that unfavorable interactions can

be accommodated by coordinating inter- and intramolecular movements suggest that structural modifications that affect the kinetics of part of a triglyceride molecule relative to its other parts, or of a molecule relative to other molecules, could be crucial regulators of triglyceride transformations. Furthermore, change can occur readily in an otherwise stable population if molecular motion is synchronous throughout the population. Triglyceride polymorphism thus becomes as much as event oriented process as it is a thermodynamically compelled process.

The modeling results for the particular structures and mode of transformation considered herein establish a theoretical basis for multiple polymorphs. Although modeling does not yet confirm exact structures, mechanisms or subcell arrangements, it defines parameters of the polymorphism problem and identifies areas for innovative research.

REFERENCES

1. Hagemann, J.W., and J.A. Rothfus, *J. Am. Oil Chem. Soc. 60*:1308 (1983).
2. Hagemann, J.W., and J.A. Rothfus, *Ibid. 65*:638 (1988).
3. McAllister, J., N. Yathindra and M. Sundaralingam, *Biochemistry 12*:1189 (1973).
4. Govil, G., R.V. Hosur and A. Saran, *Chem. Phys. Lipids 21*:77 (1978).
5. Hosur, R.V., A. Saran and G. Govil, *Indian J. Biochem. Biophys. 16*:165 (1979).
6. Kreissler, M., B. Lemaire and P. Bothorel, *Biochim. Biophys. Acta 735*:12 (1983).
7. Larsson, K., *Ark. Kemi. 23*:1 (1965).
8. Hoerr, C.W., *J. Am. Oil Chem. Soc. 41*:4, 22, 32, 34, July (1964).
9. Lutton, E.S., and A.J. Fehl, *Lipids 5*:90 (1970).
10. Larsson, K., *Fette, Seifen, Anstrichm. 74*:136 (1972).
11. Hagemann, J.W., W.H. Tallent and K.E. Kolb, *J. Am. Oil Chem. Soc. 49*:118 (1972).
12. Hagemann, J.W., and J.A. Rothfus, *Ibid. 60*:1123 (1983).
13. Larsson, K., *Chem. Scr. 1*:21 (1971).
14. Coiro, V.M., E. Giglio, A. Lucano and R. Puliti, *Acta Crystallogr. B29*:1404 (1973).
15. Lutton, E.S., *J. Am. Oil Chem. Soc. 48*:245 (1971).
16. Larsson, K., *Ark. Kemi. 23*:35 (1965).
17. Hernqvist, L., and K. Larsson, *Fette, Seifen, Anstrichm. 84*:349 (1982).
18. Simpson, T.D., *J. Am. Oil Chem. Soc. 60*:95 (1983).
19. Simpson, T.D., and J.W. Hagemann, *Ibid. 59*:169 (1982).

[Received December 31, 1987; accepted April 22, 1988]